2014-05

GaSb Oxide Thermal Stability Studied by Dynamic-XPS

UTD AUTHOR(S): Stephen McDonnell, Barry Brennan, Emin Bursa and Robert M. Wallace

JVSTB Journal of Vacuum Science & Technology B

GaSb oxide thermal stability studied by dynamic-XPS

Stephen McDonnell, Barry Brennan, Emin Bursa, Robert M. Wallace, Konrad Winkler, and Peter Baumann

Citation: Journal of Vacuum Science & Technology B **32**, 041201 (2014); doi: 10.1116/1.4878940
View online: http://dx.doi.org/10.1116/1.4878940
View Table of Contents: http://scitation.aip.org/content/avs/journal/jvstb/32/4?ver=pdfcov
Published by the AVS: Science & Technology of Materials, Interfaces, and Processing

GaSb oxide thermal stability studied by dynamic-XPS

Stephen McDonnell,[a] Barry Brennan, Emin Bursa, and Robert M. Wallace[b]
Department of Materials Science and Engineering, University of Texas at Dallas, Richardson, Texas 75080

Konrad Winkler and Peter Baumann
Omicron NanoTechnology GmbH, Limburgerstr. 75, 65232 Taunusstein, Germany

(Received 3 March 2014; accepted 6 May 2014; published 22 May 2014)

The thermal decomposition of the native GaSb oxides is studied using time resolved x-ray photoelectron spectroscopy with a temperature resolution of better than 1 K. The expected transfer of oxygen from Sb-O to Ga-O before the eventual desorption of all oxides is observed. However, an initial reaction resulting in the reduction of Sb_2O_3 along with the concurrent increase in both Ga_2O_3 and Sb_2O_4 is detected in the temperature range of 450–525 K. Using the relative changes in atomic concentrations of the chemical species observed; the initial reaction pathway is proposed.
 [http://dx.doi.org/10.1116/1.4878940]

I. INTRODUCTION

GaSb is a III-V material with applications as a potential channel material for *p*-type metal–oxide–semiconductor field effect transistors,[1,2] optoelectronics in the infrared region,[3–6] quantum devices,[7] and tunnel field effect transistors.[8] Prior to application specific processing, it is often necessary to remove the GaSb native oxide, which can be quite thick. Such oxides can inhibit subsequent epitaxy and also be a source of traps for devices as a result of defect levels in the energy gap.[2,9] To achieve this, capping the surface[10] and high temperature annealing in ultrahigh vacuum (UHV)[11,12] or other reducing ambient, such as atomic hydrogen,[3,12,13] is often employed. This process has been examined in previous works but is revisited in this study with dynamic-x-ray photoelectron spectroscopy (dynamic-XPS) where the remarkable temperature resolution combined with multichannel photoelectron data acquisition enables a detailed study of the initial decomposition of the native oxide in real time.

II. EXPERIMENT

The samples [GaSb(001) Te-doped $\sim 2\text{–}6 \times 10^{17}\,\text{cm}^{-3}$ *n*-type one side polished, epi-ready wafers from MTI Corp. item number GSTa50D05C1-US] were taken as provided by the vendor and exhibit a "native" oxide without further chemical treatments. This oxide is of particular interest since it is expected to exist on any GaSb surface that is exposed to the air. The GaSb sample was mounted to a Ta sample plate by spot-welded Ta strips prior to loading into UHV. Heating in UHV was achieved by backside radiation from a pyrolytic boron nitride (PBN) heater. The sample was out gassed for ~12 h at 373 K. For XPS, a monochromated XM1000 Al Kα ($h\nu = 1486.7$ eV) source was utilized. The core-level features of Ga $2p_{3/2}$, O 1*s*, and Sb 3*d* core-levels have been monitored and recorded versus time using a 128-channel "Argus" analyzer, recently developed by Omicron Nanoscience, running the "alternating snap-shot mode" that sets the center of the kinetic energy range for the parallel detection by the analyzer, initializes the data recording, and then sets the next kinetic energy range to be analyzed for the next core-level. This approach enables rapid data acquisition of spectral regions in a fast, parallel mode under laboratory conditions. After completing all selected snap-shot energies in a defined list, the recording loop repeats for the duration of the experiment so that each energy region can be monitored with time. The dwell time for each window was 1–2 s, so the time for one complete loop of three energy regions was <20 s. To ensure high temperature resolution, the experiment was carried out by ramping the temperature from 373 K up to 893 K over a 5 h period (ramp: 104 K/h). In this manner, the temperature varies by no more than $\Delta T < 1$ K during the data acquisition of a single "loop" of energy regions, and a total of 1200 spectra from each core-level region are acquired. The parallel-detected energy range is 7.5 eV for the selected pass energy of 50 eV. With these parameters, the instrumental energy resolution is approximately 0.2 eV. To analyze the large volume of data, the fitting software CasaXPS was utilized.[14] This software allows for large quantities of data to be analyzed using fixed ranges for particular parameter variations. Experiments carried out with this type of setup are hereafter referred to as "dynamic-XPS."

For calculating the feasibility of the various reactions discussed in this work, the total energies of each side of the reaction equations are compared in a manner similar to that utilized by Liu *et al.*,[15] using available[16,17] room temperature values for ΔG (kcal/mol) of Sb_2O_3 (−151.5), Sb_2O_4 (−190.2), Sb_20_5 (−198.2), GaSb (−9.3), and Ga_2O_3 (−238.6).

III. RESULTS AND DISCUSSION

A. Qualitative analysis

1. Contour plots

Figure 1 shows the obtained spectra in "contour" format where the binding energy is plotted on the x-axis, but intensity is plotted with color coding rather than on the y-axis as is traditional for XPS. In this manner, the variations in intensities can be monitored as a function of temperature, which is plotted on the y-axis. The energy region of 1122–1115.5 eV corresponds to the Ga $2p_{3/2}$ region [Fig. 1(a)]. The original maximum

[a]Electronic mail: stephenmcd@utdallas.edu
[b]Electronic mail: rmwallace@utdallas.edu

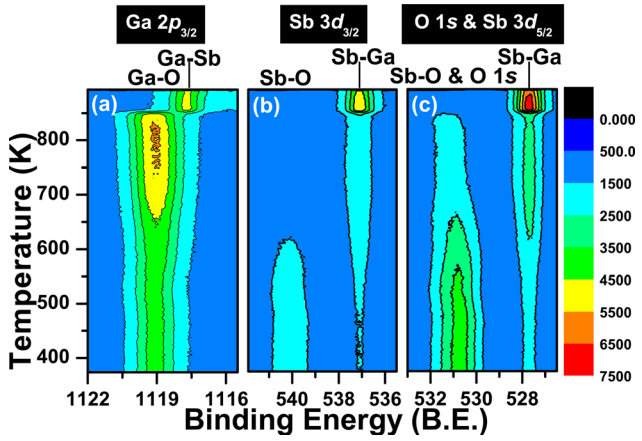

FIG. 1. (Color online) Dynamic XPS contour plot of the (a) Ga $2p_{3/2}$, (b) Sb $3d_{3/2}$, and (c) O $1s$ + Sb $3d_{5/2}$ core-level regions. The intensities are plotted with color as a function of binding energy and also sample temperature.

intensity energy position suggests oxidized gallium in the Ga_2O_3 chemical state.[2] There is an increase in intensity observed starting at ~650 K, which plateaus at ~750 K, and finally, there is complete removal of Ga_2O_3 along with the concurrent appearance of a Ga-Sb substrate signal at ~850 K. In the 542–535 eV region [Fig. 1(b)], both the oxidized antimony overlayer as well as the substrate Sb-Ga signal are observed from the sample at 373 K. At 650 K, and at the same time that the Ga_2O_3 signal is seen to increase, the Sb-O signal decreases to below the limit of detection. At approximately 850 K, the intensity of the substrate signal increases dramatically, strongly indicating the removal of an overlayer.

The 533–526 eV region [Fig. 1(c)] is slightly more complex. While the Sb $3d_{5/2}$ spectra should effectively mirror that of the Sb $3d_{3/2}$, the binding energy of the O $1s$ core level coincides with the oxidized antimony signal from the Sb $3d_{5/2}$ core level. This makes trends in the O $1s$ spectra difficult to extract, and based purely on this data shown in Fig. 1 it would appear that the oxygen signal begins to decrease at ~550 K and disappears completely at 850 K.

2. Integrated intensity as a function of temperature

In order to extract the contribution from the O $1s$ feature, one can utilize the unobstructed Sb-O feature from the Sb $3d_{3/2}$ core-level. The integrated intensity for the Sb-O features from the Sb $3d_{5/2}$ core-level should be 1.5 times the magnitude of that observed for the Sb $3d_{3/2}$ due to the electron occupancy. Using this fact, the Sb $3d_{5/2}$ contribution can be subtracted from the total feature magnitude so that the remainder can be confidently assigned to O $1s$, and this remainder is plotted as a function of temperature in Fig. 2(a). From this figure, it is clear that, other than a small decrease at 700 K, there is no significant loss of oxygen until ~850 K, which has important implications on the following oxide compositional observations since the significant desorption of oxygen containing species clearly does not occur until >700 K.

Shown in Fig. 2(b) are the areas observed for the Sb-O, Sb-Sb, Sb-Ga (GaSb substrate), and Ga-O. The results are qualitatively similar to previous reports[11,18] in that as the Sb-O features decrease the Ga-O is seen to increase, which is also similar to other reports for III-As native oxides[19–22] upon thermal annealing. This process begins at approximately 550 K and has been explained by the reaction

$$2GaSb + Sb_2O_3 \rightarrow Ga_2O_3 + 4Sb\,(-68.5\,\text{kcal/mol}), \quad (1)$$

where 4Sb thermally desorbs and the number in parenthesis is the Gibbs free energy change. This regime exists in the temperature range of 550–740 K. The desorption of Sb is not unexpected in this temperature range since Sb capping layers are reported to desorb at 573 K in UHV.[10,23]

In this work, the Ga_2O_3 is not found to desorb until the temperature range of 840–860 K, which is significantly higher than the previously reported range of 753–783 K.[11,18,24] Other than potential errors in temperature measurements between the various studies, at least two possible explanations exist to account for these discrepancies. It is possibly due to differences in the annealing environment since the previous work utilized anneals in flowing[18] H_2 or flux[24] of Sb. Another potential explanation is that in the previous studies[11,18,24] the samples were brought to, and held at, a fixed temperature for a specific time interval before cooling to room temperature for analysis, rather than being dynamically ramped as has been done in this study. It is also

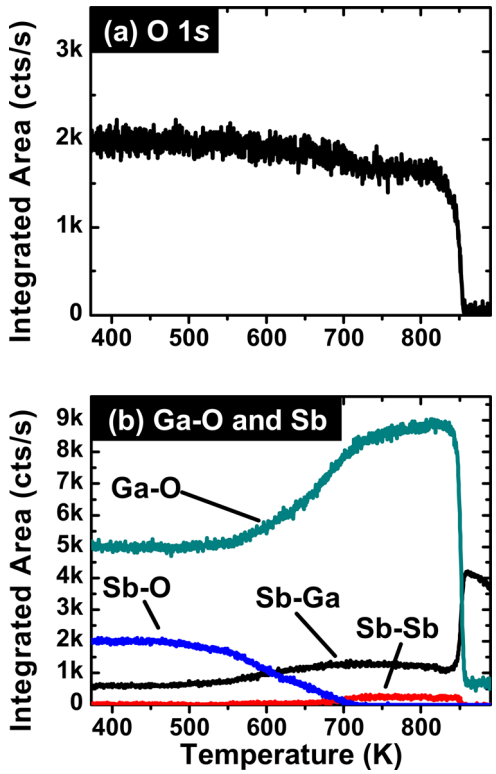

FIG. 2. (Color online) (a) Extracted O $1s$ area as a function of temperature assuming that the contributions from the Sb-O feature in the Sb $3d_{5/2}$ core-level are 1.5 times those in the Sb $3d_{3/2}$ region. This plot shows that the oxygen concentration remains effectively constant with only a small reduction at ~700 K. (b) Extracted areas for the chemical signatures of Sb-Ga (substrate), Sb-Sb, Sb-O, and Ga-O. This plot confirms the transfer of oxides from Sb to Ga and the eventual decomposition of the Ga-O at ~850 K.

interesting to note that there is a gradual increase in the Ga_2O_3 intensity between 700 K and 840 K. Since this coincides with the small reduction in the O 1*s* area, it is presumed that this increase in intensity is due to the removal of C-O species that originate in adventitious carbon on the starting surfaces. Such species have been shown to begin desorbing at temperatures of 630 K on GaAs, 670 K on AlN, and 770 K on GaN.[25,26]

B. Quantitative analysis

1. Spectral deconvolution of the Sb $3d_{3/2}$ core-level feature

The combination of the chemical analysis with 1 K temperature resolution, which is presented here, allows for more detailed information to be obtained about the initial reactions. This can be emphasized in Fig. 3(a) where the Sb $3d_{3/2}$ core-level spectra at 450 and 525 K have been isolated. It is clear from these spectra that the Sb-O feature is narrower at 525 K due to the loss of intensity on the low binding energy side, a fact that could easily be overlooked in using only Fig. 1. This strongly suggests that the broader feature at 450 K is the product of two components. Spectral analysis [shown in Fig. 3(b)] reveals that the spectra at 450 K can be fitted with a single GaSb feature plus two oxide related features at +2.5 and +3.1 eV relative to the GaSb bulk feature. The assignment of these features has not been consistent throughout the literature, with a number of works[7,13,27,28] assigning them to Sb_2O_3 and Sb_2O_5 while others[11,29,30] have chosen to assign features from 2.8 to 3.2 eV as Sb_2O_4 rather than Sb_2O_5. While this Sb_2O_4 assignment is occasionally employed to allow oxide fitting of an Sb_2O_3/Sb_2O_5 mixture with a single component,[30] at least one study[11] has fit oxide features with two components and assigned the +2.4 eV feature to Sb_2O_3 and a +3.2 eV feature to Sb_2O_4, which would appear to satisfy a simple 0.8 eV per electron charge transfer argument.

In this work, the feature at +3.1 eV with respect to the bulk is assigned to Sb_2O_4, and the reasons for this assignment will become apparent later. Fitting the spectra acquired

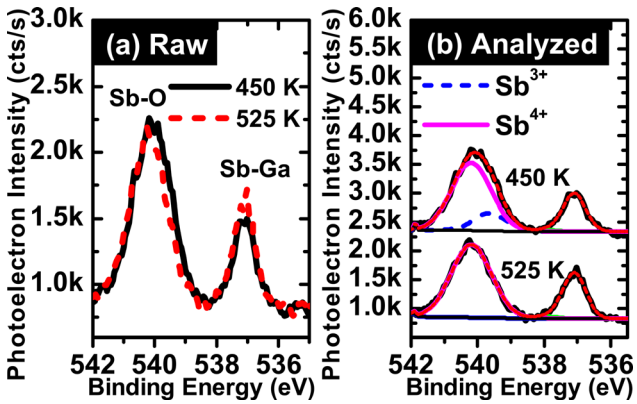

FIG. 3. (Color online) (a) Sample Sb $3d_{3/2}$ spectra taken at 450 K and 525 K, which highlight the narrowing of the feature on the low binding energy side of the oxide peak. (b) Spectral analysis of this same data showing that this narrowing is due to the removal of the low binding energy chemical state ($Sb_2O_4 + Ga_2O_3$), suggesting that it is converted to an alternative oxidation state ($Sb_2O4 + Ga_2O_3$).

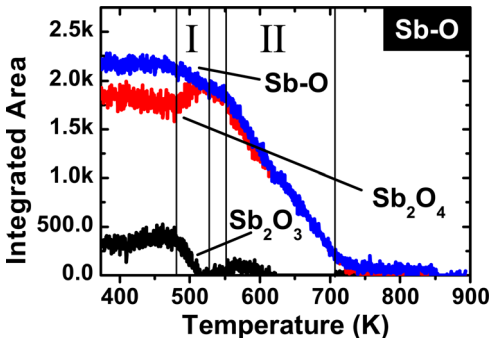

FIG. 4. (Color online) Area vs temperature plots for the deconvolved Sb $3d_{3/2}$ spectra, which highlight the presence of two distinct regions. Region II corresponds to the expected conversion of Sb_2O_3 to $Sb_2O_4 + Sb_2O_5$; however, region I is the previously unreported conversion of $Sb_2O_4 + Ga_2O_3$.

at 525 K and fixing the relative positions of the features shows a significant reduction in the Sb_2O_3 feature with a concurrent increase in the Sb_2O_4 feature compared to the spectra at 450 K. The temperature range over which this happens is highlighted as region I in Fig. 4. It appears that Sb_2O_3 is completely decomposed in this temperature range and at least some is converted to Sb_2O_4. Such a process is not explained by reaction (1).

2. Evolution of chemical states as a function of temperature

The evolution of the relative intensities for these chemical states is shown for the entire temperature ranges studied in Fig. 4. Here, it can be seen that changes take place over specific temperature ranges, designated as regions I and II in this figure. During region I, which takes place in the range of 480–530 K, the Sb_2O_4 gradually increases as the Sb_2O_3 decreases to the limit of detection. This change occurs ~40 K lower than the earliest reactions that were previously reported[11] and highlights how the improved temperature resolution provided by dynamic-XPS can reveal new information even for previously studied systems.

In the absence of an oxygen source, such a reaction necessarily requires the formation of Sb and while a small Sb feature can be detected both before and after this reaction, the change is negligible. As such, it can be inferred that the majority of the formed Sb is volatile and desorbs at these temperatures. Simply comparing the Gibbs free energies of $4Sb_2O_3 \rightarrow 3Sb_2O_4 + 2Sb$ would suggest that Sb_2O_3 is the more favorable configuration, and as such, the experimentally observed increase in Sb_2O_4 with the concurrent decrease in Sb_2O_3 likely has a more complex reaction path, as shall be discussed after considering the Ga $2p_{3/2}$ core-level spectra. As discussed in regard to Fig. 2, region II begins at 550 K, after the Sb_2O_3 concentration is decreased to the limit of detection and the Sb_2O_4 begins to decrease in intensity. This decrease can be explained by a reaction similar to reaction (1), although one should consider that the reaction does not actually start with Sb_2O_3 and so likely takes the form

$$8GaSb + 3Sb_2O_4 \rightarrow 4Ga_2O_3 + 14Sb\,(-309.4\,\mathrm{kcal/mol}). \quad (2)$$

Turning to the Ga 2*p* spectra in Fig. 2(b), it can be seen that, while the main increase in intensity occurs at 550 K coinciding with the reduction of the total Sb-O concentration (region II), from ~480 K and above, there is a gradual increase in the Ga_2O_3 feature. Again, in the absence of oxygen, the oxidation of gallium requires the scavenging of oxygen from the oxidized antimony. It can be shown that the conversion of Sb_2O_3 or Sb_2O_4 to Ga_2O_3 is favorable through a reaction with the GaSb by either reaction (1) or reaction (2). However, when considering both the increase in Ga_2O_3 and Sb_2O_4 along with the decreasing Sb_2O_3 an alternate reaction can be considered,

$$5Sb_2O_3 + 2GaSb \rightarrow 3Sb_2O_4 + Ga_2O_3 + 6Sb\,(-33.1\,\text{kcal/mol}). \quad (3)$$

This is also thermodynamically favorable and explains well the general trends observed from the XPS analysis. More interestingly, a similar expression for the conversion of Sb_2O_3 to Sb_2O_5 is not energetically favorable, showing instead an increase in energy of 94.4 kcal/mol,

$$6Sb_2O_3 + 2GaSb \rightarrow 3Sb_2O_5 + Ga_2O_3 + 8Sb\,(+94.4\,\text{kcal/mol}). \quad (4)$$

As such, the experimental observation of this decrease in the +2.4 eV Sb $3d_{3/2}$ feature along with the increase in the +3.1 eV feature serves as justification for the assignment of the +3.1 eV feature as Sb_2O_4 rather than Sb_2O_5.

More quantitatively, this reaction suggests that for every two Sb_2O_3 molecules that are decomposed, only one Sb_2O_4 is created. Given the large degree of noise in the XPS spectra, quantitative analysis is better achieved by taking the average of the peak areas within the temperature ranges. The changes in peak areas for the Sb_2O_3 and Sb_2O_4 features correspond to a 95% decrease and 10% increase in the total peak areas, respectively, and as such are well within XPS detection limits. Comparing the range of 450–480 K with the range of 510–540 K (just before and after region I), it can be found that there is a drop in the average counts of Sb_2O_3 of 124, with a concurrent increase in counts of Sb_2O_4 of 58 in reasonable agreement with the expected two to one ratio assuming the proposed reactions. Such direct comparisons of the integrated intensities for Sb_2O_3 and Sb_2O_4 are possible assuming that electrons generated from atoms in each chemical state have approximately the same photo-ionization cross sections and electron attenuations lengths. The former is approximately true since the electrons originate from the same core-level, and the latter is true since the kinetic energies of these electrons are 947 and 946.5 eV for electrons from the Sb_2O_3 and Sb_2O_4 chemical states, respectively.

This is particularly interesting in light of previous reports[12] that suggested that the decrease in Sb-O and increase in Ga-O was due to a two part reaction, viz., $2Sb_2O_5 \rightarrow Sb_2O_3 + 2O_2 \rightarrow Sb_4\uparrow + 5O_2$, $4GaSb + 3O_2 \rightarrow 2Ga_2O_3 + Sb_4\uparrow$. Clearly, if Sb_2O_3 is being removed prior to the removal of Sb_2O_4, then the reaction path is likely similar to pathway (3) above. It is also interesting to note that an increase in Sb_2O_5 was observed after annealing InSb to 525 K and was attributed to either reaction of Sb_2O_3 with H_2O or a conversion of Sb_2O_3 to Sb_2O_5.[31] Given the current state of affairs regarding the correct assignment of the +3.1 eV chemical state in the Sb $3d_{3/2}$ core-level feature, it is possible that a conversion to Sb_2O_4 was also occurring in that work. Using the Ga 2*p* core-level to quantitatively compare the increase (of 75 counts) in Ga_2O_3 species with the decrease in Sb_2O_3 during region I is possible but less precise than the earlier comparisons of Sb_2O_3 and Sb_2O_4. Accounting for the differences in photoionization potential (assumed to be proportional to the differences in the relative sensitivity factors of 3.34 and 3.07, respectively), a normalized increase of 22 counts is observed in the Ga_2O_3. This increase corresponds to 1.5% increase in the total Ga_2O_3 signal and as such is just above the limit of XPS detection. More importantly, when this value of 22 is compared to the observed decrease of 124 in Sb_2O_3, it is in good agreement with the expected 5:1 ratio for $Sb_2O_3\downarrow$:$Ga_2O_3\uparrow$.

IV. SUMMARY AND CONCLUSIONS

In summary, the application of dynamic-XPS to study the thermal desorption of native oxides on GaSb has done more than simply confirm previous findings of oxygen transfer from Sb_2O_x to Ga_2O_3 prior to the eventual complete desorption of the Ga_2O_3. Additional information about the initial reactions has been obtained, particularly in the temperature range of 480–510 K. Through reactions with the substrate and desorption of Sb, Sb_2O_3 is converted to Sb_2O_4 along with some Ga_2O_3. Simple comparison of the Gibbs free energies for these reactions would suggest that the conversion is from Sb_2O_3 to Sb_2O_4 rather than to Sb_2O_5, which strengthens the case for the assignment of the core-level feature separated +3.1 eV from the bulk Sb-Ga as Sb_2O_4 rather than Sb_2O_5 in the Sb 3*d* core level spectra for GaSb native oxides. This work has demonstrated the usefulness of dynamic-XPS and suggests that a great deal of information may be gathered even from material systems that have been previously studied by other techniques.

ACKNOWLEDGMENTS

The authors would like to acknowledge H. Dong for useful discussions. This work was supported by the Semiconductor Research Corporation Focus Center on Materials Structures and Devices (MSD), and by the Nanoelectronics Research Initiative (NRI) SWAN Center with the National Institute for Standards and Technology (NIST).

[1]A. Nainani *et al.*, *Proceedings of the 2010 IEEE International Electron Devices Meeting (IEDM)*, 2010 (unpublished).
[2]S. McDonnell, D. M. Zhernokletov, A. P. Kirk, J. Kim, and R. M. Wallace, Appl. Surf. Sci. **257**, 8747 (2011).
[3]K.-K. Lee, K. Doyle, J. Chai, J. H. Dinan, and T. H. Myers, J. Electronic Mater. **41**, 2799 (2012).
[4]A. Salesse, A. Joullié, P. Calas, J. Nieto, F. Chevrier, Y. Cuminal, G. Ferblantier, and P. Christol, Phys. Status Solidi C **4**, 1508 (2007).
[5]G. Houston, Y. Chen, J. Singleton, N. Mason, and P. Walker, Semicond. Sci. Technol. **12**, 1140 (1997).

[6]F. Chen, G. Liu, Z. Wei, R. Deng, X. Fang, S. Tian, Y. Zou, M. Li, and X. Ma, *Proceedings of the 2012 International Conference on Optoelectronics and Microelectronics (ICOM)*, 2012 (unpublished).
[7]M. V. Lebedev, E. V. Kunitsyna, W. Calvet, T. Mayer, and W. Jaegermann, J. Phys. Chem. C **117**, 15996 (2013).
[8]A. W. Dey, B. M. Borg, B. Ganjipour, M. Ek, K. A. Dick, E. Lind, C. Thelander, and L.-E. Wernersson, IEEE Electron Device Lett. **34**, 211 (2013).
[9]A. Ali *et al*., Appl. Phys. Lett. **97**, 143502 (2010).
[10]D. M. Zhernokletov, H. Dong, B. Brennan, J. Kim, R. M. Wallace, M. Yakimov, V. Tokranov, and S. Oktyabrsky, J. Vac. Sci. Technol., A **31**, 060602 (2013).
[11]Z. Lu, Y. Jiang, W. Wang, M. Teich, and R. Osgood, J. Vac. Sci. Technol., B **10**, 1856 (1992).
[12]E. Weiss, O. Klin, S. Grossman, S. Greenberg, P. Klipstein, R. Akhvlediani, R. Tessler, R. Edrei, and A. Hoffman, J. Vac. Sci. Technol., A **25**, 736 (2007).
[13]T. Veal, M. Lowe, and C. McConville, Surf. Sci. **499**, 251 (2002).
[14]N. Fairley, see http://www.casaxps.com.
[15]Z. Liu, B. Hawkins, and T. Kuech, J. Vac. Sci. Technol., B **21**, 71 (2003).
[16]R. C. Weast, D. R. Lide, M. J. Astle, and W. H. Beyer, *CRC Handbook of Chemistry and Physics*, 70th ed. (CRC, Boca Raton, FL, 1989–1990).
[17]O. Salihoglu, A. Muti, K. Kutluer, T. Tansel, R. Turan, C. Kocabas, and A. Aydinli, J. Appl. Phys. **111**, 074509 (2012).
[18]C. J. Vineis, C. A. Wang, and K. F. Jensen, J. Cryst. Growth **225**, 420 (2001).
[19]C. Y. Su, I. Lindau, P. R. Skeath, P. W. Chye, and W. E. Spicer, J. Vac. Sci. Technol. **17**, 936 (1980).
[20]C. L. Hinkle *et al*., Appl. Phys. Lett. **91**, 163512 (2007).
[21]F. S. Aguirre-Tostado, M. Milojevic, C. L. Hinkle, E. M. Vogel, R. M. Wallace, S. McDonnell, and G. J. Hughes, Appl. Phys. Lett. **92**, 171906 (2008).
[22]B. Brennan and G. Hughes, J. Appl. Phys. **108**, 053516 (2010).
[23]M. Dumas, M. Nouaoura, N. Bertru, L. Lassabatere, W. Chen, and A. Kahn, Surf. Sci. **262**, L91 (1992).
[24]L. G. Zazo, M. Montojo, J. Castano, and J. Piqueras, J. Electrochem. Soc. **136**, 1480 (1989).
[25]R. Vasquez, B. Lewis, and F. Grunthaner, Appl. Phys. Lett. **42**, 293 (1983).
[26]S. King, J. Barnak, M. Bremser, K. Tracy, C. Ronning, R. Davis, and R. Nemanich, J. Appl. Phys. **84**, 5248 (1998).
[27]D. M. Zhernokletov, H. Dong, B. Brennan, M. Yakimov, V. Tokranov, S. Oktyabrsky, J. Kim, and R. M. Wallace, Appl. Phys. Lett. **102**, 131602 (2013).
[28]D. M. Zhernokletov, H. Dong, B. Brennan, J. Kim, and R. M. Wallace, J. Vac. Sci. Technol., B **30**, 04E103 (2012).
[29]V. Bermudez, J. Appl. Phys. **114**, 024903 (2013).
[30]E. R. Cleveland, L. B. Ruppalt, B. R. Bennett, and S. Prokes, Appl. Surf. Sci. **277**, 167 (2013).
[31]M. V. Lebedev, M. Shimomura, and Y. Fukuda, Surf. Interface Anal. **42**, 791 (2010).